Supporting Information to

Gated Thermoelectric Sensation by Nanochannels Grafted with Thermally Responsive Polymers

*Shanshan Liu, Rongjie Yang, Xingyu Lin and Bin Su**

Table of Contents

S1. Materials and Reagents

2-(2-methoxyethoxy) ethyl methacrylate (MEO_2MA, M_r = 188 g/mol), oligo (ethylene glycol) methacrylate (OEGMA, M_r = 475 g/mol), benzophenone (BP) and *N*, *N*'-methylene bis(acrylamide) (MBAAm) were purchased from Aladdin. Ethanol, potassium chloride (KCl), sodium hydroxide (NaOH) were bought from Sinopharm. MEO_2MA and OEGMA were purified by a basic alumina oxide column prior to use. Other chemicals and reagents were used as received without further purification. All aqueous solutions were prepared with ultrapure water (18.2 MΩ) unless otherwise stated. Ion-tracked PET membrane (12 μm in thickness; 10^8 ion tracks/cm^2) was purchased from Wuwei Keji Xinfa.

S2. Fabrication and Characterization of PET and PET-PMO

The conical nanochannels were prepared with PET membrane, which was irradiated at the linear accelerator UNILAC (GSI, Darmstadt) with swift heavy ions (Au). The energy of each nucleon was 11.4 MeV. After UV irradiation for 1 h on each side, the membrane was chemically etched from one side contacted with 9 M NaOH at 30 °C, whereas the other side contacted with 1 M KCl and 1 M HCOOH for neutralizing the etchant.[S1] A voltage of 1 V was applied across the membrane and the ionic current was measured to control the etching process. When the current reached 10^{-8} A, the etching process was stopped.[S2] A typical *I-t* curve was shown in **Fig. S1**. The prepared PET film was immersed in Milli-Q water (18.2 MΩ) to remove the residual salt.

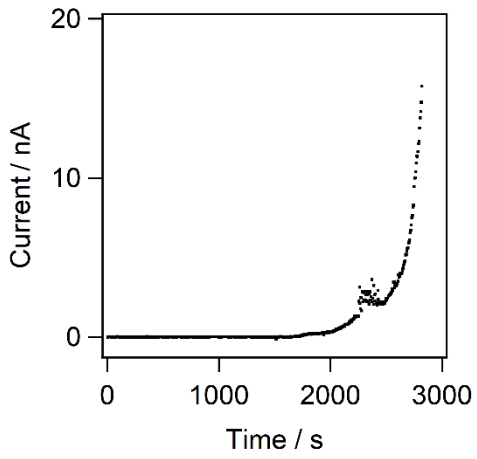

Fig. S1 *I*−*t* curve of the PET membrane upon chemical etching.

We then fabricated the PET-PMO membrane by UV grafting approach as previously reported.[S3] An ethanol solution containing MEO_2MA, OEGMA, photoinitiator (BP, n_{BP} = (n_{MEO_2MA} + n_{OEGMA}) * 0.01) and crosslinking agent (MBAAm, n_{MBAAm} = n_{BP} * 0.4) was applied to the base side of PET film by spin

coating and the molar ratio of OEGMA and MEO_2MA was varied (1 : 4 (1.1 mmol : 4.4 mmol), 1 : 7 (1.1 mmol : 7.7 mmol), 1 : 9 (1.1 mmol : 9.9 mmol), 1 : 15 (1.1 mmol : 16.5 mmol), 1 : 18(1.1 mmol : 19.8 mmol), respectively). The rotating speed was maintained at 500 rpm for 9 s and then 2000 rpm for 30 s. The PET membrane with monomer solution was placed on a temperature control table (Chemat Technology, KW-4AH) at 50 °C and irradiated under ultraviolet light (365 nm) for 30 min to obtain PET-PMO. Then it was soaked in ethanol for 24 h to remove the unreacted monomers and initiators.

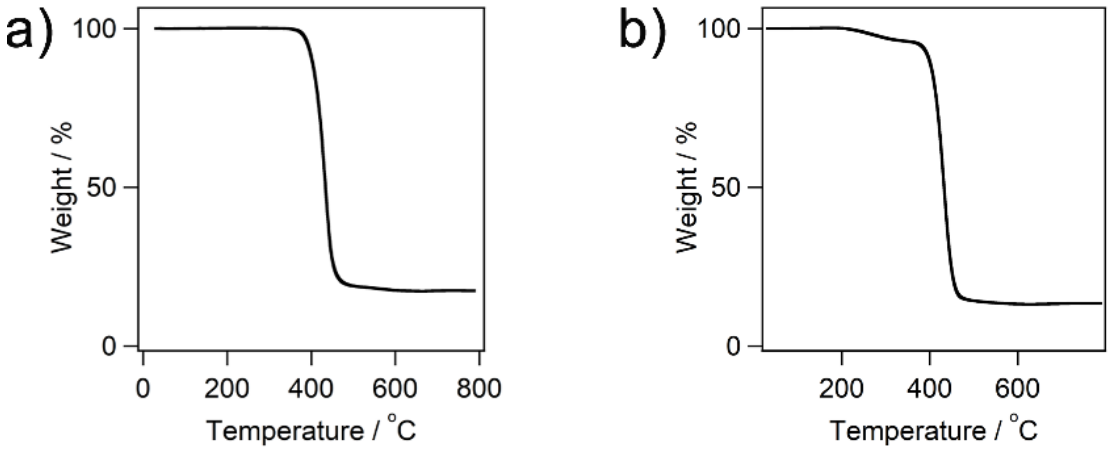

Fig. S2 TGA curves of (a) PET and (b) PET-PMO under N_2 atmosphere. The heating rate is 10 °C/min.

The thermal stabilities of PET and PET-PMO under nitrogen atmosphere were investigated, and their thermogravimetric analysis (TGA) curves were shown in **Fig. S2**. It can be observed clearly that there was only one decomposition process around 400 °C for bare PET in nitrogen atmosphere, while two loss steps with onset at 200 °C and 400 °C were observed with PET-PMO,

inconsistent with that reported in literatures.[S4, 5] From the first step, we estimated that the content of PMO was about 3%.

S3. Current and Potential Measurements

Keithley picoammeter (Keithley Instruments, Cleveland, 6847) was employed to measure the ionic current across the membrane. The membrane was mounted in between two halves of a conductivity cell. Both sides of the membrane were filled with 10 mM KCl. As shown in **Fig. S3**, the current of PET reached up to 16.1 nA which was four times larger than that of PET-PMO when the voltage was 1 V. It was reasonable because after modification the uncharged PMO decreased the surface charge density of PET. It was also in agreement with the distinct decline observed in the rectification ratio R (I_{+1V} / I_{-1V}), from 4.83 to 2.64.

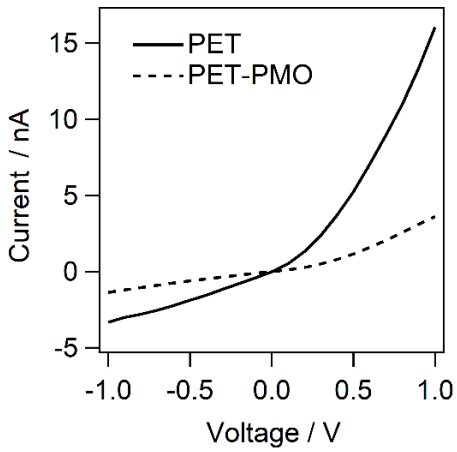

Fig. S3 *I*−*V* curves of the PET and PET-PMO membrane recorded in 10 mM KCl in a voltage range from −1 to 1 V.

The thermoelectric response was recorded by a homemade apparatus (as shown in **Fig. S4**). The micro ceramic heater (Zhuhai Huiyou Electronics) was used for heating one side of solution (tip side of PET or PMO side of PET-PMO in 10 mM KCl) by connecting with a DC power (Ningbo Jiuyuan Electronics,

QJ6003S). A temperature recorder (THMA temperature recorder, Tenghui Wenkong Instruments) was employed to measure the temperature in real time with two temperature microsensors (Tenghui Wenkong Instruments, PT100). The trans-nanochannel potential was carried out simultaneously with an Autolab electrochemical workstation (Metrohm, PGSTAT302N) by a pair of Ag/AgCl electrodes.

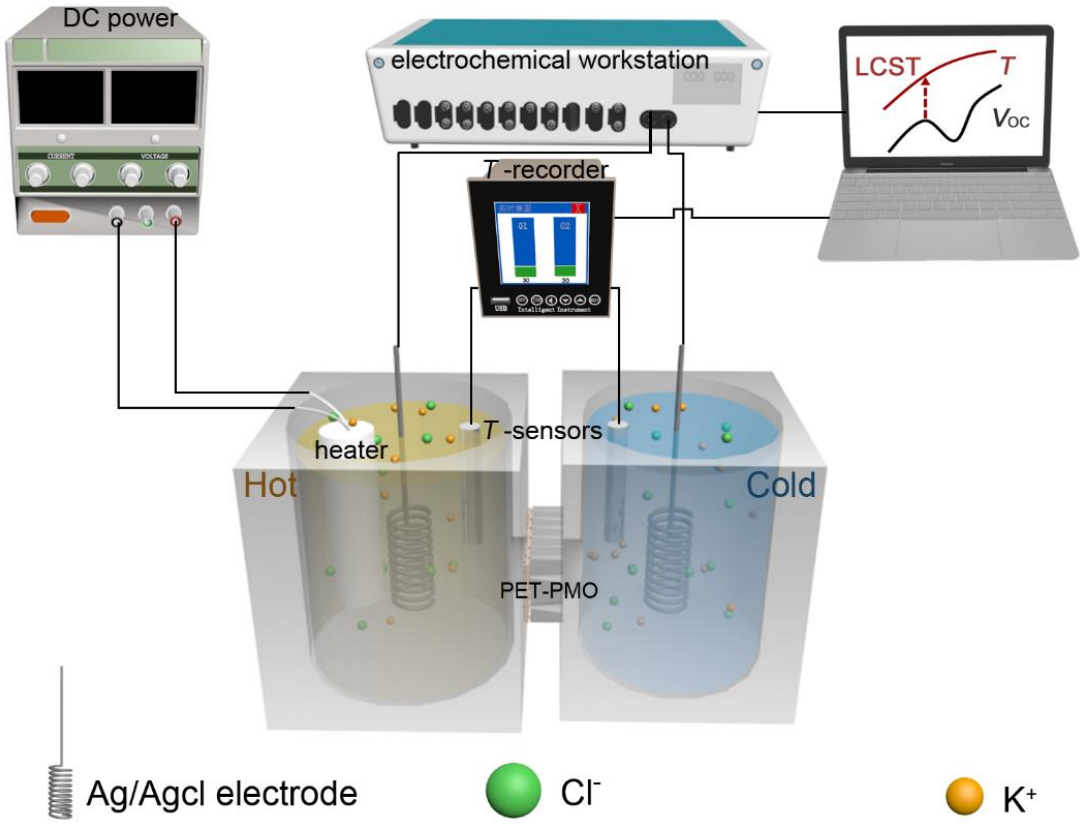

Fig.S4 Schematic illustration of the experimental apparatus for temperature control/measurement and open circuit potential recording.

S4. Theoretical Calculation of Thermoelectric Response

Theoretical calculation of thermoelectric response has been reported recently.[S6] First, the difference of redox potentials of a pair of Ag/AgCl electrodes (designated as E_{redox}) could be calculated by the following equation,

$$E_{redox} = \frac{R}{F}\Delta T \ln c \qquad \text{(S1)}$$

And the E_{redox} could be also measured by the homemade apparatus (**Fig. S4**). When ΔT reached 10 °C, E_{redox} was calculated to be about 3.97 mV by Eq. S1 with two AgCl/Ag electrodes immersed in 10 mM KCl (pH = 5.9), which coincided with the measured value.

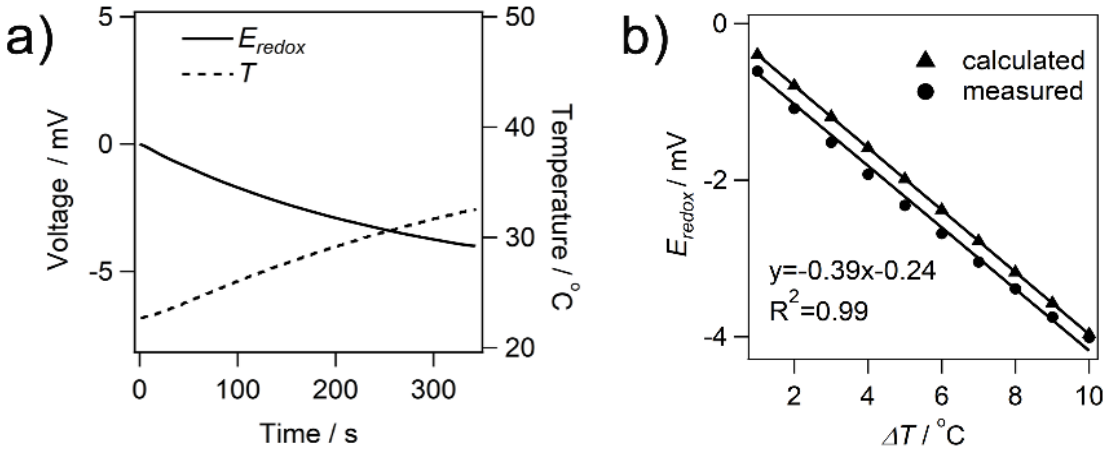

Fig. S5 (a) Synchronous time evolution curves of T and E_{redox} of a pair of Ag/AgCl electrodes. (b) A comparison of calculated (▲) and measured (•) E_{redox} as a function of ΔT.

And the trans-membrane potential was defined as ϕ and its positive direction was from the cold side to the hot side,

$$\phi = (2t_+ - 1)\frac{R}{F}\Delta T \ln c \qquad \text{(S2)}$$

During the course of the experiment, ϕ varied with temperature. If neglecting other factors, the open circuit voltage was expressed by the following equation,

$$V_{oc} = -(E_{redox} + \phi) \tag{S3}$$

Considering **Eq. S1** and **Eq. S2**, we finally obtained,

$$V_{oc} = -2t_{+}\frac{R}{F}\Delta T \ln c \tag{S4}$$

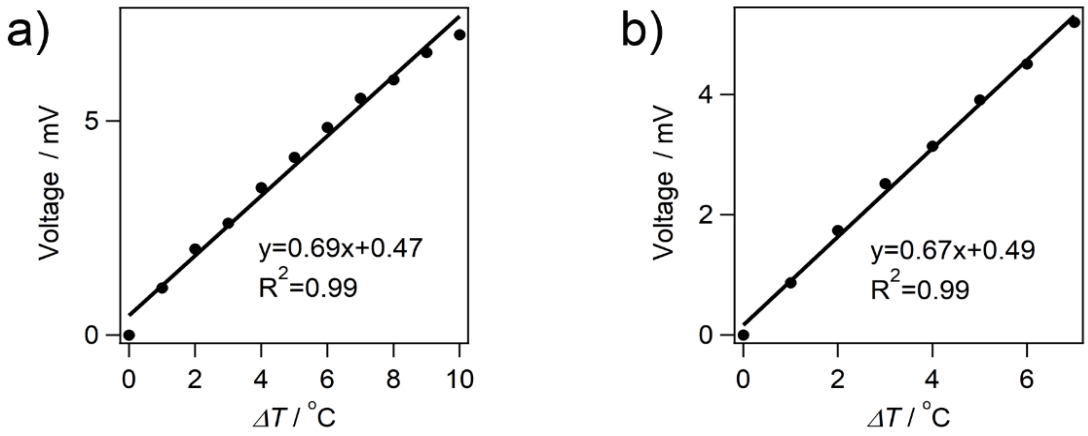

Fig. S6 The dependence of V_{oc} on ΔT.(a) PET (b) PET-PMO

Then t_+ of bare PET was calculated by **Eq. S4** and the slope of the **Fig. S6a**. In the same way, we got t_+ of PET-PMO by **Eq. S4** and the slope of the **Fig. S6b**.

S5. Influence of Coverage Ratio

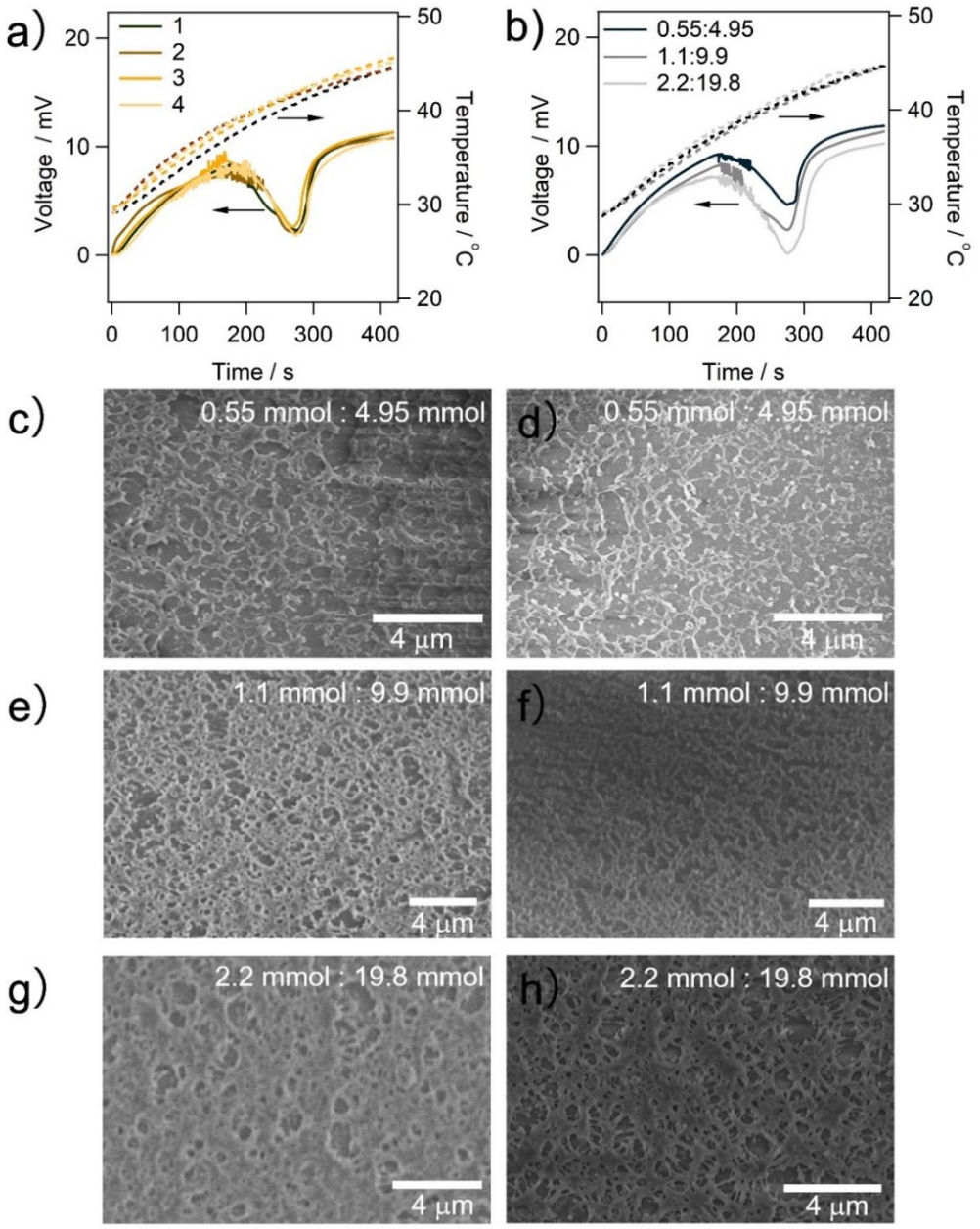

Fig. S7 (a) Synchronous time evolution curves of T and V_{oc} of four PET-PMO membranes in 10 mM KCl. And n_{OEGMA} : n_{MEO_2MA} was 1.1 mmol : 9.9 mmol. (b) Synchronous time evolution curves of T and V_{oc} of PET grafted with PMO consisting of different concentrations of MEO_2MA and OEGMA in 10 mM KCl. The surface SEM images of PET grafted with PMO consisting of different concentrations of MEO_2MA and OEGMA, n_{OEGMA} : n_{MEO_2MA} was: (c, d) 0.55 mmol : 4.95 mmol, (e, f) 1.1 mmol : 9.9 mmol, (g, h) 2.2 mmol : 19.8 mmol.

In order to prove the reliability of experimental results, parallel experiments have been done (**Fig. S7a**). We changed the concentrations of two monomers to adjust the coverage ratio that is related to the open circuit voltage response to temperature (**Fig. S7b**). When the concentrations of OEGMA and MEO_2MA were varied, the coverage ratio of PMO was estimated from the surface SEM images of PET-PMO membranes. To decrease the error in the evaluation, we made use of two surface SEM images of different membranes prepared under the same experimental conditions and took the average of them. With the lowest concentrations of OEGMA and MEO_2MA, the coverage ratio was 56.6% (an average value of 56.7% (**Fig. S7c**) and 56.4% (**Fig. S7d**)). When the concentrations of two monomers were doubled and quadrupled, the coverage ratio changed to be 73.3% (an average value of 73.4% (**Fig. S7e**) and 73.2% (**Fig. S7f**)) and 82.5% (an average value of 82.4% (**Fig. S7g**) and 82.3% (**Fig. S7h**)).

S6. Influence of Electrolyte Concentration and pH

All above experiments were carried out in the same electrolyte solution (10 mM KCl). In the following experiments, we changed the concentration (**Fig. S8a**) and pH (**Fig. S8b**) to investigate the effect of electrolyte on the response behavior. As shown in **Fig. S8a**, the values of LCST gradually diminished with the increase of electrolyte concentration. For track-etched PET, the isoelectric point (IEP) of the surface was 3.8,[S7] so the PET -PMO membrane was negatively charged when pH value was over 3.8 (PMO is neutral). Moreover, the higher pH, the larger the cation selectivity (**Fig. S8b**).

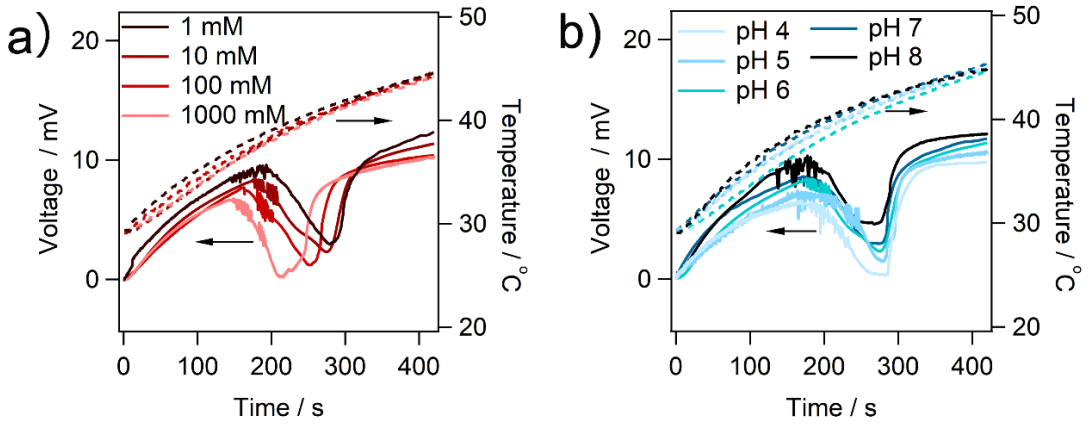

Fig. S8 (a) Synchronous time evolution curves of T and V_{oc} of PET-PMO membrane measured at different electrolyte concentrations (KCl solution). (b) Synchronous time evolution curves of T and V_{oc} of PET-PMO membrane measured at different pH values (using 10 mM KCl as electrolyte). And n_{OEGMA} : n_{MEO_2MA} was 1.1 mmol : 9.9 mmol

S7. Characteristics of PET Grafted with PMO on Base Side

For comparison, PMO was also grafted onto the base surface of PET. The LCST was also 37 °C due to the same molar ratio of PMO (**Fig. S9a**). Its morphology was shown in **Fig. S9b**. The surface was covered with a discontinuous PMO layer. Since the diameter of channels were so large that PMO could not cover all the surface of the channel, the increase in the number of opening channels caused by PMO shrinkage was less than that of tip side, thus, the response to temperature was not clear.

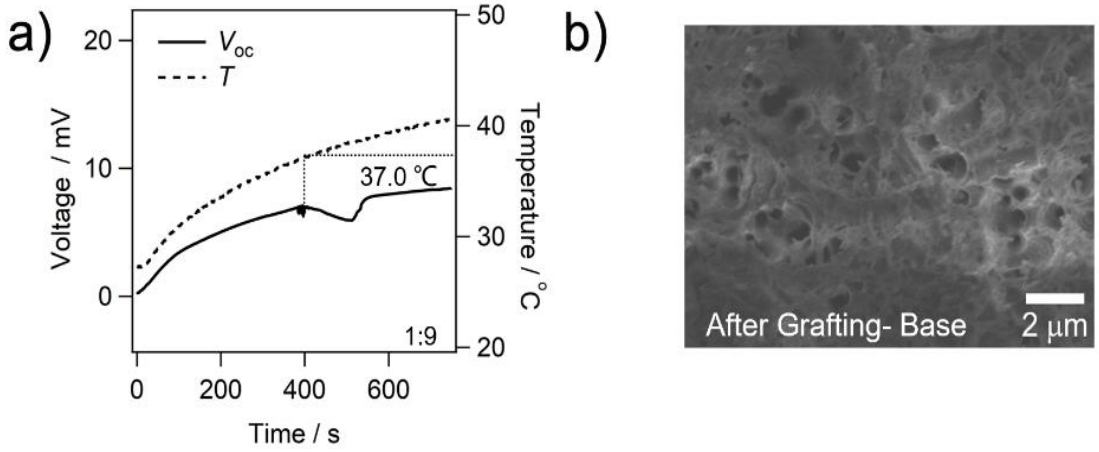

Fig. S9 (a) Synchronous time evolution curves of T and V_{oc} of PET-PMO with base grafting surfaces in 10 mM KCl. (b) The base surface SEM images of the PET-PMO membrane. And n_{OEGMA} : n_{MEO_2MA} was 1 : 9.

References

S1. Z. S. Siwy, *Adv. Funct. Mater.*, 2006, **16**, 735-746.

S2. Z. S. Siwy, M. R. Powell, A. Petrov, E. Kalman, C. Trautmann and R. S. Eisenberg, *Nano Lett.*, 2006, **6**, 1729-1734.

S3. B. Yang and W. Yang, *J. Membr. Sci.*, 2003, **218**, 247-255.

S4. A. C. Santos, A. F. M. Santos, H. P. Diogo, S. P. C. Alves, J. P. S. Farinha, N. T. Correia, M. Dionísio and M. T. Viciosa, *Polymer*, 2018, **148**, 339-350.

S5. Z.-Z. Wu, Y.-P. Ni, T. Fu, B.-W. Liu, W.-S. Wu, L. Chen, X.-L. Wang and Y.-Z. Wang, *Polymer Degradation and Stability*, 2018, **155**, 162-172.

S6. K. Chen, L. Yao and B. Su, *J. Am. Chem. Soc.*, 2019, **141**, 8608-8615.

S7. Z. Siwy, Y. Gu, H. A. Spohr, D. Baur, A. Wolf-Reber, R. Spohr, P. Apel and Y. E. Korchev, *Europhys. Lett.*, 2002, **60**, 349-355.